PROPOSED EXPERIMENTAL STUDIES FOR ASSESSING IONOSPHERIC PERTURBATIONS ON SPS UPLINK PILOT BEAM SIGNAL

Santimay Basu and Sunanda Basu
Emmanuel College
Boston, MA 02115

Introduction

The microwave beam of the proposed Solar Power Satellite (SPS) at geosynchronous altitude is to be formed and directed by phase information derived from a pilot signal at 2.45 GHz transmitted from ground and received in a number of module locations on the SPS antenna. The frequency of the pilot signal has been chosen to be sufficiently low as to avoid the effects of strong scattering by turbulence in the neutral atmosphere and yet high enough to avoid any possible refractive effects caused by the ionized upper atmosphere. However, the ionosphere is known to contain irregular variation of concentration due to natural processes and the downlink microwave beam has also been predicted to interact with the ionosphere to cause artificial irregularities (Perkins and Valeo, 1974; Perkins and Roble, 1978; Duncan and Behnke, 1978). Thus the uplink pilot signal has to propagate through the ionosphere containing natural and possibly some artificial irregularities. In view of the fact that microwave signals from communication satellites suffer considerable perturbations both in intensity and phase in the equatorial and auroral zones there has been some concern that the uplink pilot signal may suffer perturbations with possible consequences to the formation of the downlink high power microwave beam. While there may exist some satisfaction regarding the SPS site location at midlatitudes avoiding the intense belt of equatorial and auroral irregularities, there is evidence for the occurrence of ionospheric irregularities at midlatitudes causing considerable perturbations of signal intensity at VHF and even at GHz. Though these effects due to natural irregularities are usually smaller at midlatitudes as compared to the equatorial zone, the effective perturbations at midlatitudes may become magnified if a geostationary satellite acquires finite orbital inclination. The generation of artificial irregularities by ionospheric heating in the underdense mode and the effects thereof on transionospheric microwave propagation remain totally unexplored from the experimental standpoint. In the following sections we shall provide some evidence of the occurrence of natural irregularities at midlatitudes based on scintillation measurements by the use of VHF and GHz transmissions from geostationary satellites and satellite in-situ measurements. We shall then provide an outline of our proposed measurements related to the detection, lifetime and drift of artificial irregularities generated by ionospheric heating in the underdense mode.

Formulation of the Problem

Figure 1 illustrates that in the presence of fluctuations of ionospheric electron concentration confined within a layer of thickness L_e, an incident plane wave undergoes phase fluctuations as it emerges from the layer. For small phase fluctuations, the emerging wavefront contains only phase perturbations without any fluctuations in intensity. As the wavefront propagates towards the observer's plane, phase mixing occurs and thereby spatial intensity fluctuations also develop. In the presence of a relative motion between the propagation path and the irregularities, the spatial variations of intensity and phase sweep past the observer's receiving system giving rise to temporal variations in phase and intensity called phase and intensity scintillations. In the practical situation, such as for the SPS case, or radio wave scintillation measurements, the ionospheric irregularities between the transmitter and the receiver are located in the far zone of the transmitter so that the radiation can be well approximated by a spherical wave. On the other hand, the beam nature of the wave has to be considered when the irregularities are located in the near zone of the transmitter as frequently encountered in optical propagation (Ishimaru, 1978).
In the case of spherical wave propagation between a transmitter and receiver separated by a distance L and the scatterers at a variable distance η from the transmitter the correlation functions of intensity (I) and phase (ϕ) over the receiving plane in the weak-scatter regime are given by:

$$B_I(L,\rho) = \langle I(L,\rho_1) I(L,\rho_2) \rangle$$
$$= (2\pi)^2 \int_0^L d\eta \int_0^\infty \kappa \, d\kappa \, J_0(\kappa\eta\rho/L) \, |H_r|^2 \, \Phi_n(\kappa) \qquad (1)$$

$$B\phi(L,\rho) = \langle \phi(L,\rho_1)\phi(L,\rho_2) \rangle$$

$$= (2\pi)^2 \int_0^L d\eta \int_0^\infty \kappa d\kappa \, J_o(\kappa\eta\rho/L) \, |H_i|^2 \, \Phi_n(\kappa) \qquad (2)$$

where

ρ - dimension transverse to propagation path
κ - irregularity wave number
$\Phi_n(\kappa)$ - irregularity wave number spectrum
k - wave number of the propagating wave

$$|H_r|^2 = k^2 \sin^2|\eta(L-\eta)\kappa^2/2kL|$$

$$|H_i|^2 = k^2 \cos^2|\eta(L-\eta)\kappa^2/2kL|$$

The variance of intensity and phase may be obtained by putting $\rho = 0$ in equations (1) and (2). These equations may be used to obtain the respective variances from a knowledge of the irregularity spectrum. In solving the equations for the ionospheric case, it must be considered that the irregularities in the inertial subrange cause the diffraction effects as distinct from the case of geometrical optics. Measurement of variances and temporal spectra allow a determination of the strength of turbulence which may then be used to derive the structure functions of phase and intensity. In principle, direct measurements of phase and intensity correlations are possible using the spaced receiver technique with variable baselines.

Strong Ionospheric Irregularities at Midlatitudes

At Ramey Air Force base near Arecibo, Puerto Rico, nighttime scintillation events accompanied by long period (30 mins to 1 hour) variations of total electron content have been routinely observed (Kersley et al., 1979; Basu et al., 1979). The top panel in Figure 2 shows the temporal (local time = UT-4.5 hours) variations of total electron content measured with a radio polarimeter by the use of 137 MHz transmissions from geostationary satellite, SMS-1. The bottom panel shows that the fluctuations in total electron content were accompanied by intensity scintillations in excess of 15 dB.

Satellite in-situ observations have also revealed existence of such large and small scale structure near Arecibo. The solid line in Figure 3 shows the spatial variation of ion concentration, N (or electron concentration for charge neutrality at F region heights) recorded by the ion drift meter on board the Atmosphere Explorer E satellite. The AE-E data has been kindly made available to us by W.B. Hanson. The ion concentration is sampled 16 times per sec. The irregularity amplitude $\Delta N/N$ computed from 3-sec intervals of N data are indicated by the circles. The satellite altitude, longitude, magnetic local time and latitude are indicated in the diagram. Long period spatial variations of electron concentration, as well as, steep horizontal gradients at a latitude close to that of Arecibo may be noted. Such steep gradients are accompanied by small scale irregularities with amplitudes exceeding 10%. Such levels of irregularity amplitude ($\Delta N/N$) and ambient density (N) provides ΔN values which can explain observed scintillation events near Arecibo shown in Figure 2 if we assume a layer thickness of about 100 km (Basu and Basu, 1976).

In Figure 4 we show a case of similar perturbations of total electron content accompanied by 1 dB fluctuation of intensity at 1.7 GHz (Fujita et al., 1978). Such levels of GHz scintillation activity with a maximum of 2.3 dB are often observed near the June solstice at Kashima, Japan with ETS-II satellite, for which the propagation path is nearly aligned with the earth's magnetic field. It may be of interest to note that the magnetic dip location of Kashima is nearly identical to that of Arecibo although the geographic latitude is higher than Arecibo. An equivalent enhancement of scintillation activity may be encountered at U.S. sites such as, Boulder or Arecibo, if the geostationary satellite acquires finite orbital inclination. Such large amplitude natural irregularities may cause phase perturbations at the SPS frequency. Their effects on both the pilot and power beams should be carefully assessed.

Proposed Measurement of Phase and Intensity Scintillation Effects During Ionospheric Heating

We have made plans to perform several experiments in conjunction with RF ionospheric heating both in the overdense and underdense modes at Arecibo and at Platteville. In December, 1979, we had planned to make use of the Arecibo heating facility and perform ground and airborne measurements of the effects of ionospheric heating. Figure 5 shows the observing geometry, the shaded region indicating the heated volume at 5 MHz. From Roosevelt Roads, Puerto Rico, we planned to receive the 249 MHz transmissions from LES-9 and obtain the variance and temporal spectra of phase and intensity scintillations at that frequency. In view of the finite orbital inclination of LES-9 satellite, the locus of the intersection of the propagation path with 300 km ionospheric height lies within the heated volume between 06-10 UT. In addition, the AFGL Airborne Ionospheric Observatory agreed to provide supporting measurements of phase and intensity scintillations using LES-9 and Fleetsatcom satellites (Figure 5) 6300 Å airglow and ionosonde measurements. The Fleetsatcom satellite was chosen to probe the ionosphere outside the heated volume and detect the presence of naturally occurring irregularities. The aircraft was also expected to scan the heated region to define the extent of the perturbed volume. Simultaneous diagnostic incoherent scatter measurements from Arecibo Observatory were requested for determining the electron concentration and temperature.

Unfortunately, the Arecibo Heating Facility could not be made operational in December, 1979 so that the above experiments had to be postponed. However, we have drawn up a back-up plan for similar experiments using the LES-8 satellite in conjunction with the heating facility at Platteville during Feb-March, 1980 (Rush et al., 1979). In addition to some of the experiments outlined above, we have planned to include spaced receiver scintillation measurements to obtain ionospheric drift. We also propose to set up an observing station such that a field aligned propagation path can be viewed through the heated volume. These measurements will provide an estimate of the phase and intensity structure functions. Experimental support for the above program will be provided by Dr. J. Aarons of AFGL. At a later date, we shall utilise the phase coherent spread spectrum signals from NAVSTAR-GPS satellites at 1575 MHz and 1227 MHz to make accurate phase scintillation measurements in the GHz range. These results are expected to provide a direct input to the design of the SPS system. However, it is essential that the heating facilities at Arecibo and Platteville be upgraded as proposed by Gordon and Duncan (1978) and Rush et al., (1979) to meet the SPS power density levels at F-region altitudes before accurate experimental results can be provided for predicting SPS ionospheric and telecommunication systems impact.

This work was partially supported by National Science Foundation Grant No. ATM 78-25264 and Air Force Geophysics Laboratory Contract F19628-78-C-0005.

References

Basu, S. and S. Basu, Geophys. Res. Lett., 3, 681, 1976.

Basu, S., S. Basu, S. Ganguly and J.A. Klobuchar, Simultaneous Incoherent Scatter and Scintillation/Total Electron Content Observations in the Mid-latitude Ionosphere, presented at National Radio Science Meeting, URSI, Boulder, Colorado, November, 1979.

Duncan, L.M. and R.A. Behnke, Phys. Rev. Lett., 41, 998, 1978.

Fujita, M., T. Ogawa and K. Koike, J. Atmos. Terr. Phys., 40, 963, 1978.

Gordon, W.E. and L.M. Duncan, NASA Report No. NAS9-15212, July, 1978.

Ishimaru, A., Wave Propagation and Scattering in Random Media, Academic Press, New York, 1978.

Kersley, L., J. Aarons and J.A. Klobuchar, J. Geophys. Res., 1979 (in press).

Perkins, F.W. and E.J. Valeo, Phys. Rev. Lett., 32, 1234, 1974.

Perkins, F.W. and R.G. Roble, J. Geophys. Res., 83, 1611, 1978.

Rush, C.M., J.C. Carroll and E.J. Violette, Report No. NTIA-TM-79-27, U.S. Dept. of Commerce, October, 1979.

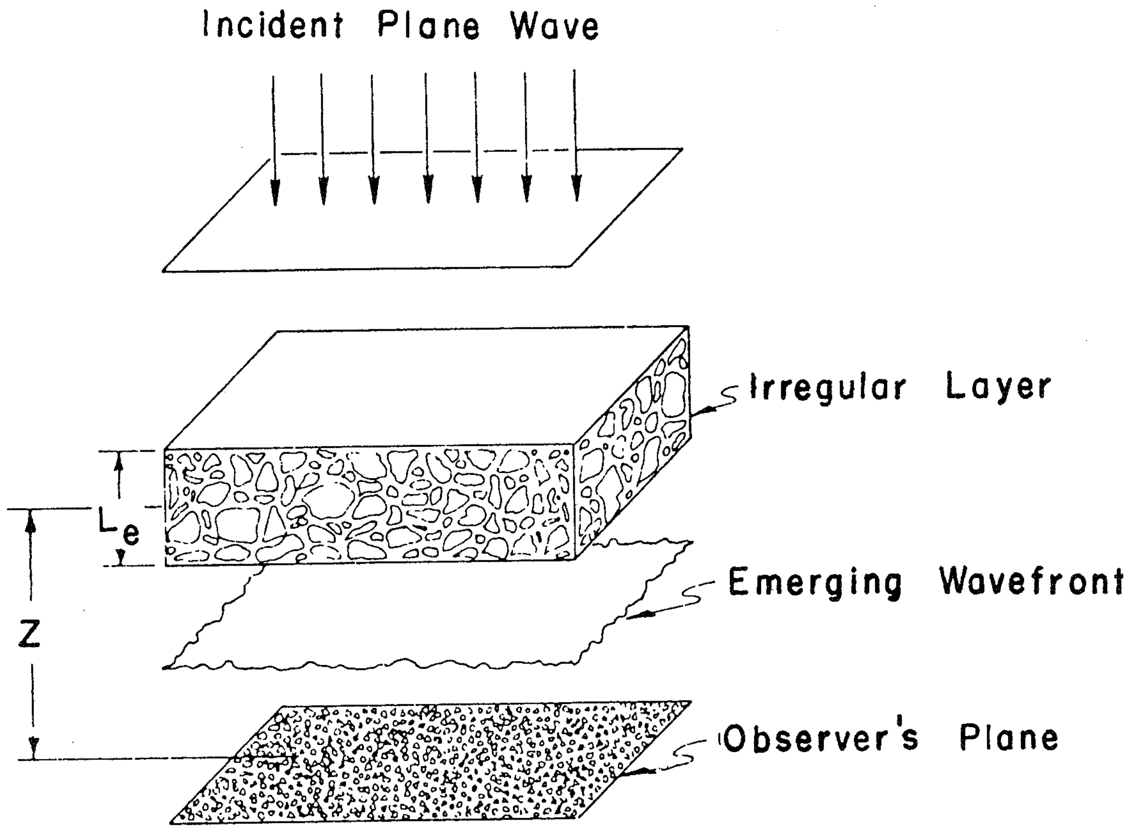

Figure 1. Geometry of the scintillation problem.

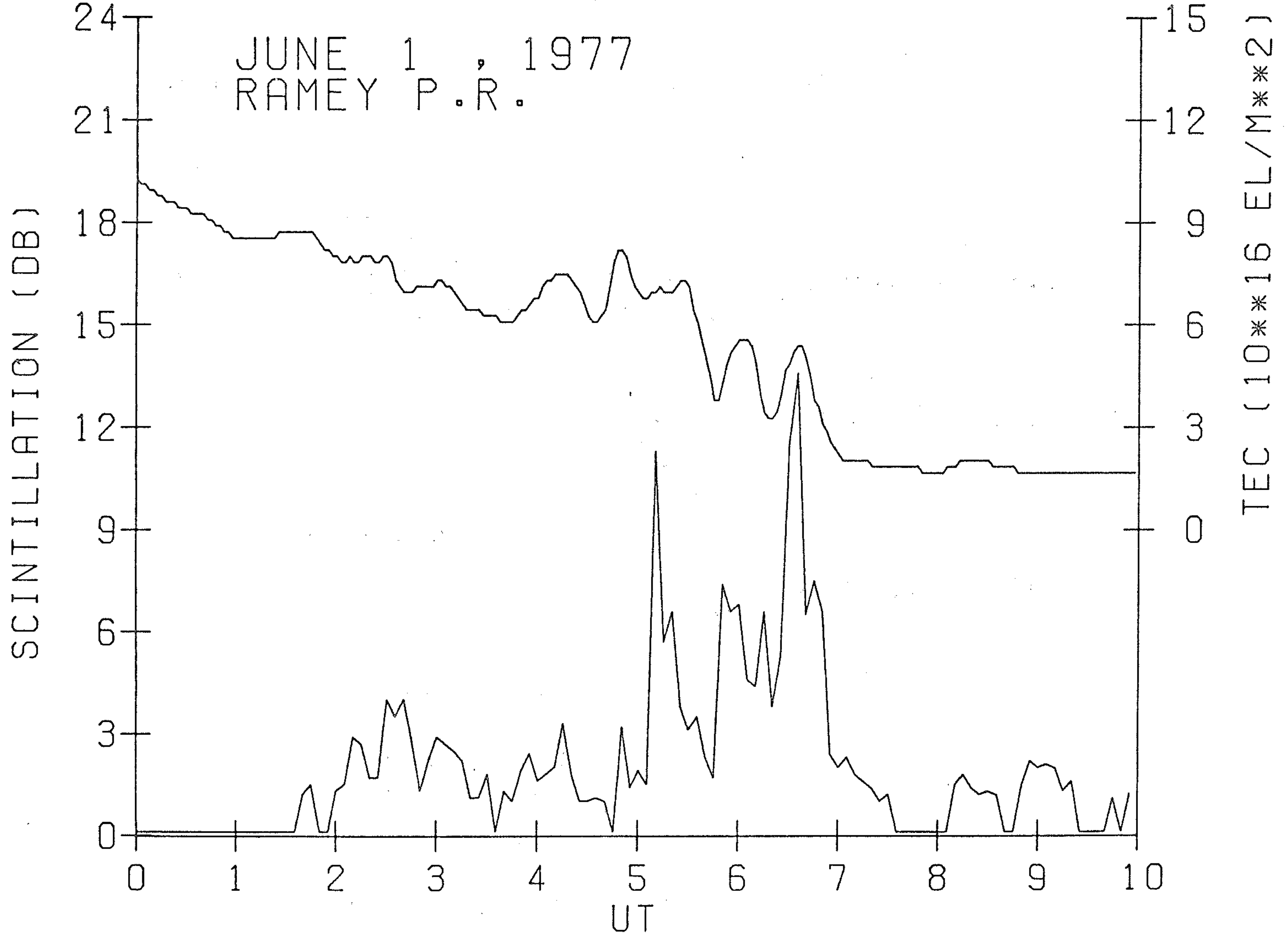

Fig. 2. Total electron content (top panel) and scintillation (lower panel) measurements obtained at Ramey Air Force Base, P.R., using SMS-1 at 137 MHz on June 1, 1977 showing large amplitude scintillations correlated with content fluctuations. This diagram was made available by J.A. Klobuchar of AFGL.

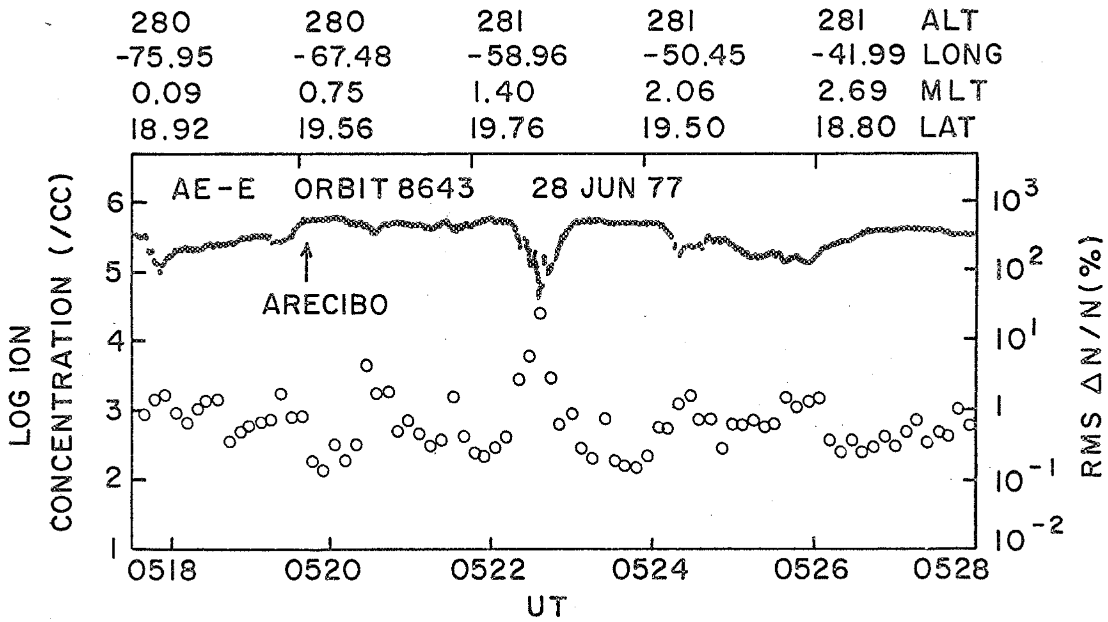

Figure 3. Atmospheric Explorer E orbit near Arecibo showing large amplitude irregularities.

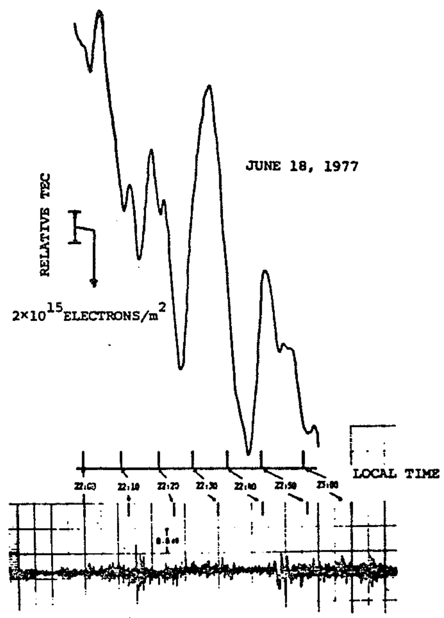

Figure 4. Example of nighttime scintillation (lower) and irregular variation of TEC (upper) observed at Kashima on June 18, 1977.

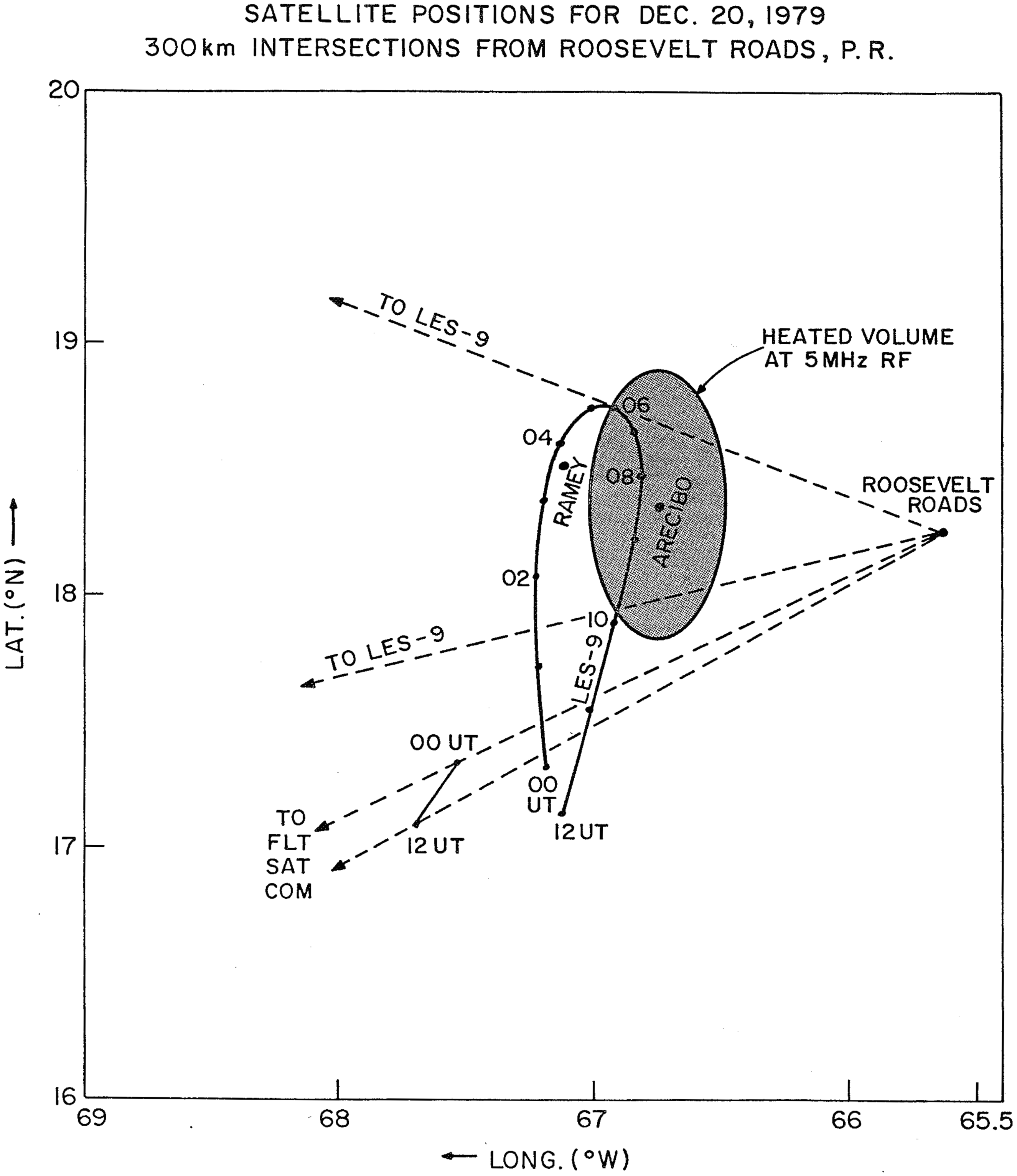

Figure 5. Observing geometry of LES-9 and Fleetsatcom satellites during proposed ionospheric heating from Arecibo.

CONCLUSIONS PRESENTED AT THE SYSTEM PERFORMANCE SESSION

1. Performance Based on System Sizing

   a. Reduced power levels (< 5GW) will have only small degradations in microwave transfer efficiency.

   b. Antennas with less than 1 Km diameter at 2450 MHz quickly degrade in microwave transmission efficiency as the size decreases.

2. Antenna Illumination - a 10-step, 10dB gaussian taper is the optimum antenna illumination for rectenna collection efficiency, given the 21 kW/m^2 and 23 mW/m^2 constraints.

3. Antenna/Subarray Mechanical Alignments

   a. Antenna/subarray mechanical alignment is constrained by the allowable peak grating lobe levels (assumed to be $\leq$ .01 mW/cm^2) and the allowable scattered power levels.

   b. Antenna alignment is constrained to $\leq$ 1 min. for phase control at the 10-meter per side subarray size and $\leq$ 3 min. for phase control to the power module (tube) level (average 3 meters per side subarray size).

   c. The subarray size of 10m X 10m, based on microwave system requirements, represents a good compromise between conflicting mechanical and electronic requirements. Larger subarrays (e.g. 18m X 18m) would require motor-driven screwjacks, whereas smaller subarrays (e.g. 4m X 4m) would complicate the phase control electronics and construction and maintenance requirements.

4. Startup/Shutdown Operations - Three possible sequences for antenna startup/shutdown operations will provide sidelobe peak levels outside of the rectenna boundaries less than those experienced during normal steady-state operations.

5. Sources of Scattered Microwave Power - The greatest contributors to lost or scattered microwave power are, in order of importance:

   - Tube failures - 268 MW, based on a maximum of 2% tube failures at any one time
   - Phase errors - 188 MW, based on 10° RMS phase error
   - Subarray tilt - 188 MW, based on ± 3 min. subarray misalignment
   - Amplitude error - 67 MW, based on ± 1dB amplitude error across the surface area fed by one klystron tube
   - Antenna tilt - 27 MW, based on ± 1 min. antenna misalignment
   - Subarray spacings - 6.7 MW, based on 0.25-inch gap spacing between mechanical subarrays.

SYSTEM PERFORMANCE CONCLUSIONS (CONTINUED)

6. Initial theoretical studies indicate that Faraday rotation induced by the ionosphere will not be a problem.

REMAINING ISSUES - ENVIRONMENTAL - PRESENTED AT THE SYSTEM PERFORMANCE SESSION

1. Validity of the present ionospheric transmission limit of 23 mW/cm^2
2. Effects of heating/disturbing the ionosphere on communications
3. Effects of heating/disturbing the ionosphere on performance of microwave system
4. Electromagnetic compatibility
   a. Radiated noise/harmonics at SPS
   b. Reradiated noise/harmonics at rectenna